Fluid Phase Equilibria 275 (2009) 52–59

Contents lists available at ScienceDirect

Fluid Phase Equilibria

journal homepage: www.elsevier.com/locate/fluid

Solubility of hydrocarbons in water: Experimental measurements and modeling using a group contribution with association equation of state (GCA-EoS)

Selva Pereda[a], Javeed A. Awan[b], Amir H. Mohammadi[b], Alain Valtz[b], Christophe Coquelet[b], Esteban A. Brignole[a], Dominique Richon[b,*]

[a] Planta Piloto de Ingeniería Química, Universidad Nacional del Sur, CONICET, CC 717, 8000 Bahía Blanca, Argentina
[b] MINES ParisTech, CEP/TEP - Centre énergétique et procédés, CNRS FRE 2861, 35 Rue Saint Honoré, 77305 Fontainebleau, France

ARTICLE INFO

Article history:
Received 5 June 2008
Received in revised form
10 September 2008
Accepted 11 September 2008
Available online 21 September 2008

Keywords:
GCA-EoS
Equation of state
Water
Hydrocarbon
Phase equilibria
Experimental measurement
Normal hexane
Cyclo-hexane and Iso-octane

ABSTRACT

In this communication, new experimental data on the solubility of n-hexane, cyclo-hexane and iso-octane in pure water are reported. The data have been measured using a static-analytic technique that takes advantage of a Rolsi™ sampling device in the temperature range of 298–353 K and at pressures up to 0.5 MPa. The experimental data measured in this work at 298 K have been compared with some selected data from the literature and good agreement is found. A group contribution plus association equation of state, namely the GCA-EoS, is used to model the phase equilibrium of water + hydrocarbon (C_2 to n-C_6, cy-C_6, i-C_4 and i-C_8) system. The predictions of the model are found in good agreement with the experimental data measured in this work and some selected data from the literature.

1. Introduction

Petroleum fluids are normally saturated with water in the reservoirs. During production, transportation, and processing opeartions, the dissolved water in the hydrocarbon phase may condense. The condensed water may contribute to gas hydrates and/or ice formation at specific temperatures and pressures. This phenomenon can arise during transportation in pipelines with large temperature gradients. The formation of gas hydrates and/or ice could result in the blockage and shutdown of pipelines. Forming a condensed water phase may also lead to corrosion and/or two-phase flow problems [1,2]. To avoid these problems, accurate knowledge of water + hydrocarbon phase behavior is of interest to the petroleum industry [1,2]. Estimating water + hydrocarbon phase behavior is also crucial in the design and operation of natural gas facilities [1,2]. The hydrocarbon solubility in water is also an important issue from an environmental standpoint, due to new legislations and restrictions on the hydrocarbon content in water disposal [2]. Unfortunately, experimental data on the solubility of heavy hydrocarbons in water, especially at low temperatures are scarce and often scattered [1,2]. This is partly due to the fact that the solubility of heavy hydrocarbons in water is indeed very low and hence generally very difficult to measure. Modeling these systems is also very difficult due to their extreme non-ideal behavior, *i.e.* the mutual solubilities in the existing phases are generally different by several orders of magnitude and present completely dissimilar behavior. The very low solubility of hydrocarbons in water typically presents a minimum value at low temperatures, while the solubility of water in hydrocarbons increases monotonically with temperature.

The existing thermodynamic models typically use cubic equations of state (CEoS) for modeling the fluid phase(s), where the association and solvatation effects are normally ignored. These effects play an important contribution to the non-ideality of fluid mixtures, such as the systems containing water. A well-known concept applied in modeling associating solutions is the chemical theory [3,4], which postulates the existence of distinct chemical species in solution. A different approach is to apply statistical-mechanics such as Wertheim's perturbation theory [5,6] for fluids with highly oriented attractive forces. Wertheim's theory has been

* Corresponding author. Tel.: +33 1 64 69 49 65; fax: +33 1 64 69 49 68.
E-mail address: richon@ensmp.fr (D. Richon).

0378-3812/$ – see front matter © 2008 Elsevier B.V. All rights reserved.
doi:10.1016/j.fluid.2008.09.008

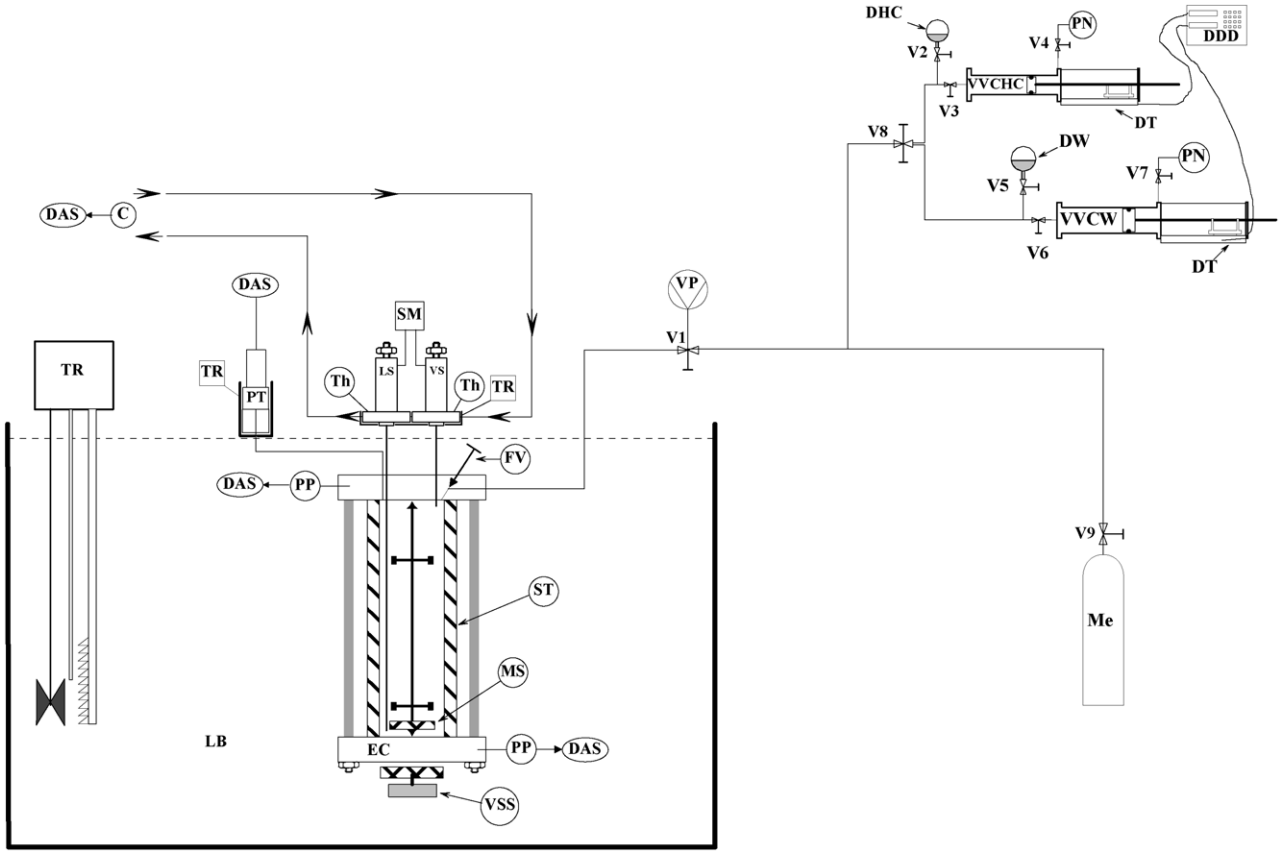

Fig. 1. Schematic picture of the apparatus. C, carrier gas; DAS, data acquisition system; DW, degassed water; DDD, displacement digital display; DHC, degassed hydrocarbon; DT, displacement transducer; EC, equilibrium cell; FV, feeding valve; LB, liquid bath; LS, liquid sampler; Me, methane cylinder (for pressurizing system); MS, magnetic stirring; PN, pressurized nitrogen; PP, platinum temperature probe; PT, pressure transducer; SM, sampler monitoring; ST, sapphire tube; Th, thermocouple; TR, temperature regulator; VS, vapor sampler; VSS, variable speed stirring; VVCHC, variable volume cell for hydrocarbons; Vi, shut-off valve; VP, vacuum pump; VVCA, variable volume cell for aqueous solution.

used in equations of state like the statistical associating fluid theory (SAFT) [7,8], the cubic plus association (CPA) equation of state [9–11] and the group contribution associating (GCA) equation of state [12–14].

Zabaloy et al. [12] and Economou and Tsonopoulos [15] used models that explicitly accounted for association (GCA-EoS, SAFT and associated-perturbed-anisotropic-chain-theory APACT) to describe phase behavior of water + hydrocarbon systems. Later, Voutsas et al. [16] and Yakoumis et al. [17] reported comparisons between the capabilities of SAFT and CPA for modeling the mutual solubility in water + hydrocarbon system. In general, all these works do a good job in predicting the water content of the hydrocarbon phase while the prediction of the hydrocarbon content of the water phase is less accurate. CPA performs better but still presents important deviations in the water phase hydrocarbons solubilities. Recently, Oliveira *et al.* [18] presented a review of the most important works in the literature on the modeling mutual solubility of water + hydrocarbon systems. In the same work, they showed the ability of CPA to model the liquid–liquid equilibrium (LLE) of water + hydrocarbon system for a large number of compounds.

The goal of this work is to provide new experimental data on the solubilities of some heavy hydrocarbons in water and to study the capability of a GCA-EoS to model phase behavior of water + hydrocarbon system. For this purpose, we first report new experimental data on the solubility of normal hexane, cyclo-hexane and iso-octane (2,2,4-trimethyl-pentane) in water, which have been measured using a static-analytic technique that takes advantage of a Rolsi™ sampling device [19]. The experimental data measured in this work at 298 K are compared with some selected experimental data from the literature. Using equilibrium data reported in this work and in the literature, the parameters of GCA-EoS [12,13] were adjusted and are reported here. The model predictions are finally compared with some selected experimental data from the literature.

2. Experimental

Cyclo-hexane and n-hexane were purchased from Merck with purities of 99%, while iso-octane (2,2,4-trimethyl pentane) was purchased from Fluka Chemie with a 99.5% purity.

The experimental method used in this work is a "static-analytic" type. A schematic picture of the corresponding equipment is given in Fig. 1. The experimental procedure is the same one described by Valtz et al. [19]. Analyses were performed using a gas chromatograph (VARIAN model CP-3800) equipped with dual thermal conductivity detectors (TCD1 and TCD2) and a flame ionization detector (FID).

The Pt 100 Ω temperature probes were calibrated, following ITS 90, against a 25 Ω reference platinum temperature probe (TINLEY Precision Instrument) fitted with an eight-digit multimode (Hewlett Packard 34420A). Uncertainty was estimated to be ±0.01 K for the Pt 100 Ω platinum temperature probes.

A Druck model (PTX 611) pressure transducer was used in this work, which was thermoregulated at a fixed temperature (higher than the working temperature to avoid any condensation phenomena). The calibration was performed against a pressure calibration

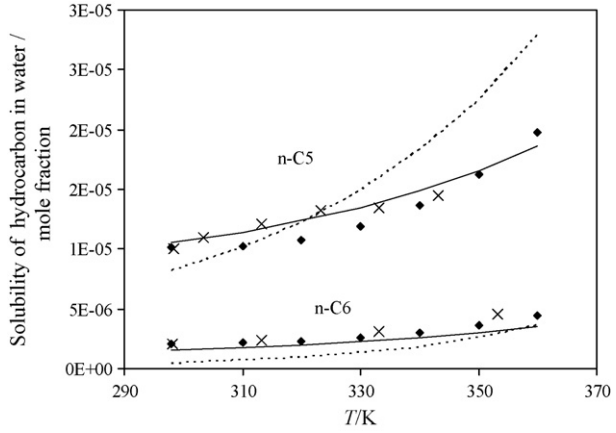

Fig. 2. Effect of temperature dependence of hard sphere diameter of water (d_w) on the solubility of hydrocarbon in aqueous phase. Dashed curves: predictions using original d_w (Eq. (1)). Solid curves: predictions using new temperature dependency for d_w (Eq. (2)). Data: (×) Mokraoui [31], (♦) Tsonopoulos [25].

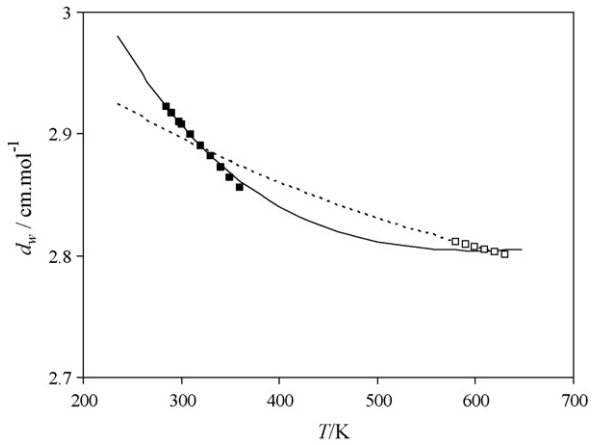

Fig. 3. Temperature dependency for water hard sphere diameter. Symbols are the values used to perform the least-square fitting to get Eq. (2). (■) d_w values to get the correct temperature dependency of hydrocarbon solubility in pure water. (□) d_w values from original d_i Eq. (1) to get correct d_w at high temperatures. Solid curve: new temperature dependency for water hard sphere diameter. Dashed curve: original temperature dependency for water hard sphere diameter.

device (Desgranges et Huot, France, model 24610). The uncertainty for the pressure transducer was estimated to be ±0.0001 MPa.

The FID' TCD1 and TCD2 were calibrated using set amounts of compounds injected through syringes. All the calibrations were performed for each system under study to check for any changes in the detector response coefficients. The maximum uncertainties for TCDs and FID calibrations were 2% and 1.8%, respectively.

3. Group contribution + association equation of state

The GCA-EoS model [12,13] is an extension of a group contribution equation of state, the GC-EoS, proposed by Skjøld-Jorgensen [20,21]. In this model, there are three contributions to the residual Helmholtz function: repulsive, attractive, and associative. A brief description of the GCA-EoS model is given in Appendix. This model has proven to be successful in predicting phase equilibrium of associating [13,14,22] and size-asymmetric [23,24] mixtures. In particular, vapor–liquid equilibrium (VLE) LLE, and vapor–liquid–liquid equilibrium (VLLE), conditions are adequately predicted with a single set of parameters.

A first conventional parameterization, adjusting binary interaction parameters (k_{ij}, k_{ij}, α_{ij} and α_{ji}), was performed by correlating only solubility data of n-pentane and n-hexane in water. In this case, it was possible to reproduce the order of magnitude of the hydrocarbon (C_2 to n-C_6) solubility in water. However, it was not possible to obtain the correct temperature dependence of the solubility data (a common problem for almost all models available in the literature). The model systematically gives steeper slopes of the solubility than those shown by the experimental data as it is illustrated in Fig. 2 (dashed lines) for the case of n-C_5 and n-C_6 solubilities in pure water. As LLE is highly sensitive to the hard sphere diameter parameter (d_i) of the repulsive contribution to the residual Helmholtz energy (see the model details in Appendix), we studied the effect of this variable on the mutual solubility predictions.

The original temperature dependence of d_i for all components is given by:

$$d_i = 1.065655 d_{ci}\left\{1 - 0.12\exp\left[-\frac{2T_{ci}}{3T}\right]\right\} \quad (1)$$

where T represents the temperature and d_c is the value of the hard-sphere diameter at the critical temperature, T_c, for the component i, which normally is fitted to reproduce a point of the vapor pressure curve of the pure component. This functionality of d_i with temperature was empirically proposed in the original GC-EoS [20].

As a result of this study, we concluded that the temperature dependence of the hard sphere diameter of water, d_w, has a strong influence on the temperature dependence of the hydrocarbon solubility in water. In a first step, the constant 0.12 of Eq. (1) for water was increased up to the value that gives the correct temperature dependence. This value was 0.26 (see continuous line in Fig. 2). Afterwards, a new temperature dependency was obtained only for the hard sphere diameter of water, which gives the correct slope within the temperature range of our experimental data and also ensures that at higher temperatures similar values of d_w are obtained with both Eqs. (1) and (2). The new functionality is:

$$d_w = d_{cw}\left\{0.554\left[\exp\left[-\frac{2T_{cw}}{3T}\right]\right]^2 - 0.543\exp\left[-\frac{2T_{cw}}{3T}\right] + 1.097\right\} \quad (2)$$

Fig. 3 shows the original and the new d_w temperature dependence along with the values used to perform the least-square fitting that results in Eq. (2).

To summarize, binary interaction parameters reported in this work were estimated on the basis of the data available for the solubilities of n-pentane and n-hexane in pure water. In the following section, the predictive capability of GCA-EoS is demonstrated for other linear alkanes like ethane, propane, n-butane, n-heptane and n-octane. In the case of iso-octane and cyclo-hexane, different groups than those present in linear paraffins are required to build up the molecule, those are: cyCH_2, CH_3(B) and CH(B) (see Skjøld-Jorgensen [20]) thus the solubility data was also correlated in this two cases. However, it is important to highlight that it was not necessary to fit the four interaction parameters for each pair, but only a small adjustment of one of the non-randomness parameter ($\alpha_{\text{hydrocarbon group-}H_2O}$) was performed to improve the model correlation.

Table 1
Experimental solubility of n-hexane in pure water (mole fraction), this work.

T/K	P/MPa	n	$x_{n\text{-C6}}$	$2\sigma x$
298.09	0.500	18	2.08E−06	9.00E−08
313.15	0.503	17	3.22E−06	6.00E−08
333.15	0.501	14	3.08E−06	5.00E−08
353.15	0.503	15	4.58E−06	1.00E−07

n = number of samples analyzed, x = mole fraction in aqueous phase, $\sigma_x = ((n \times \sum x^2 - (\sum x)^2)/n \times (n-1))^{1/2}$.

Table 2
Experimental solubility of cyclo-hexane in pure water (mole fraction), this work.

T/K	P/MPa	n	$x_{cy\text{-}C6}$	$2\sigma x$
298.10	0.501	12	1.25E−05	3.00E−07
313.15	0.502	12	1.34E−05	2.00E−07
333.14	0.500	11	1.68E−05	2.00E−07
353.16	0.502	11	2.43E−05	6.00E−07

n = number of samples analyzed, x = mole fraction in aqueous phase, $\sigma_x = ((n \times \sum x^2 - (\sum x)^2)/n \times (n-1))^{1/2}$.

Table 3
Experimental solubility of 2,2,4-trimethyl-pentane (iso-octane) in pure water (mole fraction), this work.

T/K	P/MPa	n	$x_{2,2,4\text{-tmp}}$	$2\sigma x$
298.15	0.501	13	3.68E−07	8.00E−08
313.15	0.499	14	3.45E−07	3.00E−08
343.16	0.440	13	7.04E−07	7.00E−08
353.15	0.500	17	1.00E−06	3.00E−08

n = number of samples analyzed, x = mole fraction in aqueous phase, $\sigma_x = ((n \times \sum x^2 - (\sum x)^2)/n \times (n-1))^{1/2}$.

Table 4
Values of n-hexane and cyclo-hexane solubilities in pure water (mole fraction) calculated using the correlation of Tsonopoulos [25].

T/K	x_{n-C_6}	x_{cy-C_6}
298.15	2.11E−06	1.27E−05
313.15	2.16E−06	1.42E−05
333.15	2.65E−06	1.80E−05
353.15	3.82E−06	2.47E−05

x = mole fraction in aqueous phase.

Table 5
Comparison of literature data and the data measured in this work for n-hexane solubility in pure water (mole fraction) at 298 K.

x_{n-C_6}	Reference
1.99E−06	Mc Auliffe [27]
3.83E−06	Nelson and de Ligny [32]
2.59E−06	Polak and Lu [33]
2.57E−06	Leinonen and Mackay [28]
2.80E−06	Krasnoshchekova and Gubergrits [34]
2.08E−06	This work

x = mole fraction in aqueous phase.

4. Results and discussion

Experimental solubility data measured in this work are given in Tables 1–3 for n-hexane, cyclo-hexane and 2,2,4-trimethyl-pentane (iso-octane), respectively. Solubility values of *n*-hexane and cyclo-hexane in pure water calculated using the correlation of Tsonopoulos [25], are reported in Table 4. The values calculated with the correlation of Tsonopoulos [25] are quite close to our measurements.

Table 6
Comparison of literature data and the data measured in this work for cyclo-hexane solubility in pure water (mole fraction) at 298 K.

x_{cy-C_6}	Reference
1.18E−05	Mc Auliffe [27]
1.71E−05	Guseva and Parnov [35]
1.21E−05	Leinonen and Mackay [28]
1.71E−05	Guseva and Parnov [36]
1.18E−05	Mc Auliffe [26]
2.14E−04	Verhoeye [37]
1.90E−05	Pierotti and Liabastre [38]
1.13E−05	Sanemasa et al. [29]
1.28E−05	de Hemptinne et al. [30]
1.25E−05	This work

x = mole fraction in aqueous phase.

Table 7
Comparison of literature data and the data measured in this work for 2,2,4-trimethyl-pentane solubility in pure water (mole fraction) at 298 K.

$x_{2,2,4\text{-tmp}}$	Reference
3.80E−07	Mc Auliffe [27]
3.20E−07	Polak and Lu [33]
3.80E−07	Mc Auliffe [26]
3.68E−07	This work

x = mole fraction in aqueous phase.

Table 8
The GCA-EoS pure-group parameters.

Group	q	T^*	g^*	g'	g''
CH_3	0.848	600.0	316,910	−0.9274	0.0
CH_2	0.540	600.0	356,080	−0.8755	0.0
CH	0.228	600.0	356,080	−0.8755	0.0
C	0.000	600.0	–	–	–
CH_3(B)	0.789	600.0	316,910	−0.9274	0.0
CH_2(B)	0.502	600.0	356,080	−0.8755	0.0
$cyCH_2$	0.540	600.0	466,550	−0.6062	0.0
i-C_4H_{10}	3.084	498.1	326,400	−0.4896	0.0
H_2O	0.866	647.3	1,383,953	−0.2493	0.0

Table 9
The GCA-EoS binary interaction parameters.

i	j	k_{ij}	k_{ij}'	α_{ij}	α_{ji}
H_2O	CH_3	0.62	−0.05	12.00	0.41
	CH_2	0.62	−0.05	12.00	0.59
	CH	0.62	−0.05	12.00	0.59
	C	–	–	–	–
	CH_3(B)	0.62	−0.05	12.00	1.05
	CH_2(B)	0.62	−0.05	12.00	0.59
	$cyCH_2$	0.62	−0.05	12.00	0.58
	i-C_4H_{10}	0.60	0.00	22.25	0.55

A comparison of our experimental data at 298 K with literature data is done in Tables 5–7. Literature data are quite scattered; our experimental data are closer to that of Mc Auliffe [26] for n-hexane, to that of Mc Auliffe [26,27], Leinonen and Mackay [28], Sanemasa et al. [29] and de Hemptinne et al. [30] for cyclo-hexane and to that of Mc Auliffe [26,27] for 2,2,4-trimethyl-pentane.

Concerning the modeling with GCA-EoS, all the components are described by group contribution, except iso-butane, which is described molecularly. Table 8 reports the pure-group parameters used in this work. Table 9 contains the values of the binary

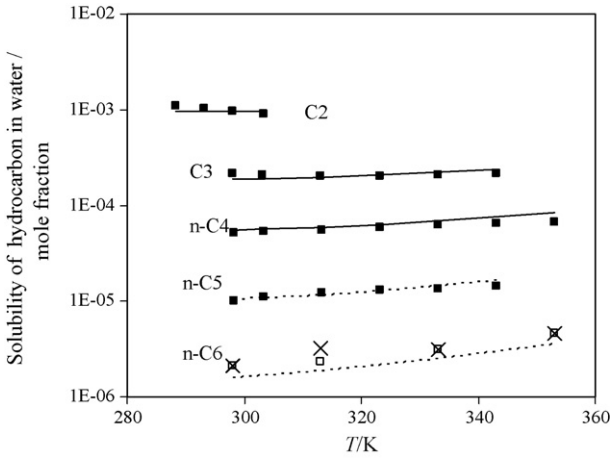

Fig. 4. Solubility of n-alkanes in pure water. Symbols: (□) and (■) experimental data from Ref. [31]; (×) new experimental data reported in this work. Curves: results of GCA-EoS model: dashed curves, correlation; solid curves, model predictions.

Table 10
Deviation of GCA-EoS model results for normal alkane solubility in pure water from corresponding experimental values [31] (values are in mole fraction).

T/K	P/MPa	$x_{exp} \times 10^4$	$x_{model} \times 10^4$	RD%
Ethane				
288.33	3.412	10.90	9.68	11.2
293.15	3.788	10.34	9.57	7.4
298.01	4.198	9.56	9.50	0.6
303.30	4.615	9.01	9.45	4.9
				AAD% = 6.0
Propane				
298.08	0.985	2.151	1.876	12.8
303.18	1.101	2.095	1.898	9.4
313.11	1.391	2.034	1.964	3.5
323.15	1.741	2.016	2.060	2.2
333.16	2.152	2.062	2.189	6.2
343.18	2.633	2.141	2.352	9.9
				AAD% = 7.3
n-Butane				
298.29	0.531	0.520	0.556	7.0
303.31	0.567	0.527	0.566	7.3
313.24	0.387	0.553	0.591	6.8
323.15	0.508	0.593	0.631	6.4
333.28	0.660	0.617	0.687	11.3
343.16	0.840	0.655	0.758	15.7
353.14	1.059	0.659	0.848	28.7
				AAD% = 11.9
n-Pentane				
298.28	0.498	0.100	0.104	3.6
303.31	0.509	0.110	0.107	3.1
313.19	0.496	0.121	0.115	5.1
323.24	0.548	0.132	0.127	4.1
333.21	0.510	0.135	0.142	5.5
343.15	0.508	0.145	0.163	12.5
				AAD% = 5.7
n-Hexane				
298.09	0.500	0.0208	0.0159	23.4
313.15	0.503	0.0233	0.0185	20.5
333.15	0.501	0.0308	0.0248	19.6
353.15	0.503	0.0458	0.0361	21.2
				AAD% = 21.2

interaction parameters between groups i and j, k^*_{ij} and k'_{ij} and the values of the non-randomness parameters α_{ij} and α_{ji}. As mentioned in the previous section, the k_{ij}, k_{ij}' and α_{ij} are the same in all the cases and only the α_{ji} is slightly different for each pair.

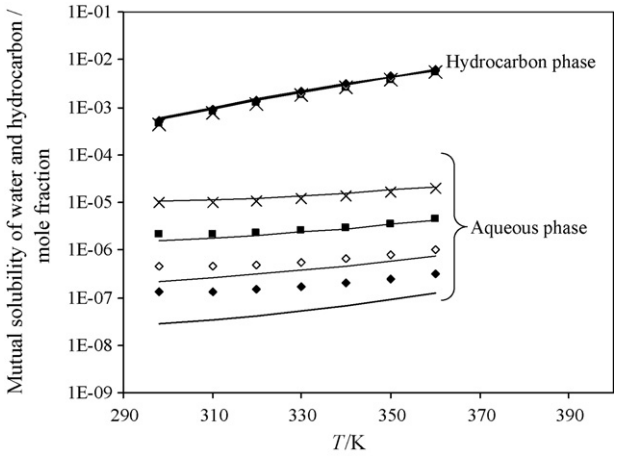

Fig. 5. Mutual solubility in heavy hydrocarbon (n-C_5–n-C_8) + water system. Symbols: pseudo-experimental values generated using correlation of Tsonopoulos [25]: (×) n-C_5, (■) n-C_6, (◊) n-C_7, (♦) n-C_8. Curves: GCA-EoS model predictions. The data on solubility of water in hydrocarbon overlap each other.

Table 11
Deviation of GCA-EoS model results for iso-butane, iso-octane and cyclo-hexane solubility in pure water from corresponding experimental values (values are in mole fraction)[a].

T/K	P/MPa	$x_{exp} \times 10^4$	$x_{model} \times 10^4$	RD%
Iso-butane				
298.23	0.354	0.96	1.00	4.5
303.33	0.411	0.97	0.98	1.4
313.30	0.540	0.99	0.97	2.4
323.21	0.697	1.00	0.97	2.8
333.24	0.890	1.02	0.99	3.4
343.19	1.120	1.03	1.02	0.9
353.14	1.391	1.04	1.08	3.7
363.19	1.712	1.05	1.16	10.6
				AAD%‡ = 3.7
Cyclo-hexane				
298.10	0.501	0.125	0.124	0.4
313.15	0.502	0.134	0.142	6.3
333.14	0.500	0.168	0.183	9.2
353.16	0.502	0.243	0.253	4.3
				AAD% = 5.1
Iso-octane				
298.15	0.501	0.00368	0.00423	15.0
313.15	0.499	0.00345	0.00468	35.7
343.16	0.440	0.00704	0.00713	1.30
353.15	0.500	0.01000	0.00866	13.4
				AAD% = 16.4

[a] Experimental data for iso-butane have been taken from Ref. [31] while experimental data for cyclo-hexane and iso-octane have been taken from Tables 4 and 5, respectively.

Fig. 4 presents the GCA-EoS model predictions for the solubilities of normal alkanes, C_2–C_4 in water along with the final model correlation of n-C_5 and n-C_6 data. Table 10 presents the experimental data selected from the literature [31], the GCA-EoS model predictions, and the relative errors for each experimental point. The results show that by using a group contribution approach, the GCA-EoS model is able to predict a change of four orders of magnitude in the solubility, going from normal hexane to ethane. Fig. 5 shows the capability of the GCA-EoS model for predicting mutual solubility of high molecular weight normal alkanes. In this case, the GCA-EoS model results are compared with the results of Tsonopoulos correlation [25] for n-C_5–n-C_8. As can be seen, the model can predict the solubility in both phases using a group contribution approach.

Table 11 reports GCA-EOS model correlation for iso-butane, cyclo-hexane and 2,2,4-trimethyl-pentane along with the relative

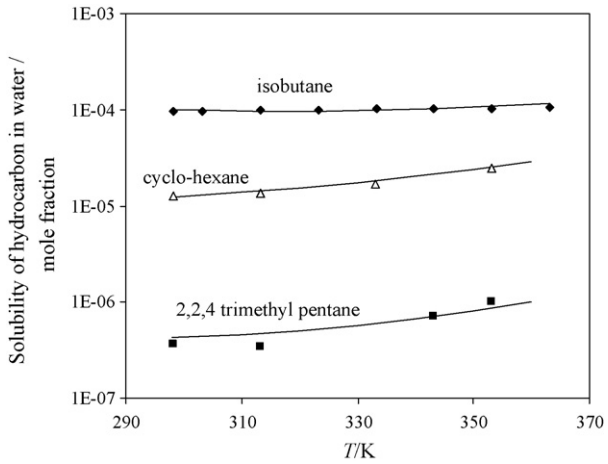

Fig. 6. Solubility of iso-butane, iso-octane and cyclo-hexane in pure water. Symbols: experimental data: (■) 2,2,4-trimethyl-pentane, this work; (Δ) cyclo-hexane, this work; (♦) iso-butane [31]. Curves: predictions of GCA-EoS model.

errors for each experimental point. Iso-butane solubility in water is one order of magnitude higher than the corresponding one of n-butane (See Tables 10 and 11). Therefore, this compound was treated molecularly (Tables 8 and 9 report the group and binary interaction parameters, respectively). On the other hand, cyclo-hexane and iso-octane were represented by group contribution. Fig. 6 shows the good agreement of GCA-EoS model predictions with the experimental data on solubilities of iso-butane, cyclo-hexane and iso-octane in pure water. To our knowledge there is no equation of state model able to describe the extremely low solubility of hydrocarbons in water with the low errors that the GCA-EoS model has shown in this work.

5. Conclusions

In this work, new experimental data on the solubility of normal-hexane, cyclo-hexane and iso-octane in pure water are reported. The measurements were performed using a static-analytic technique that takes advantage of a Rolsi™ sampling device. The experimental data measured in this work at 298 K are compared with some selected experimental data from the literature and the agreement was generally found acceptable. The GCA-EoS model was used to model the phase behavior of water + hydrocarbon system, and it showed good capability to predict the mutual solubility with relatively small deviations even at the extreme low solubility presented by the heavy hydrocarbon in water. A new expression is proposed for the hard sphere diameter of water that adequately represents the temperature dependence of the hydrocarbon solubility in water and the vapor pressure of water.

List of symbols

A	Helmholtz energy (J mol^{-1})
AAD%	average absolute deviation $(100\sqrt{\sum_N((x_{\text{model}}-x_{\text{exp}})/x_{\text{exp}})^2}/N)$
A^{assoc}	Helmholtz energy term describing association part (J mol^{-1})
A^{att}	Helmholtz energy term describing attractive part (J mol^{-1})
A^{c}	configurational Helmholtz function (J mol^{-1})
A^{fv}	Helmholtz energy term describing free volume part (J mol^{-1})
A^{ideal}	Helmholtz energy term describing ideal behavior part (J mol^{-1})
d_{ci}	hard sphere diameter of the component i at the critical temperature (cm mol^{-1})
d_i	hard sphere diameter of the component i (cm mol^{-1})
g_{ij}	attraction energy parameter for interactions between groups i and j (J cm^3 mol/[surface area segment]^2)
g'_{jj}, g''_{jj}	the GCA-EoS pure-group parameters
g^*_{jj}	the interaction parameter for reference temperature
k	Boltzman constant (J K^{-1})
k_{ij}, k'_{ij}	binary interaction parameters
k^*_{ij}	interaction parameter for reference temperature
M_i	number of associating sites assigned to group i
N	number of experimental data
NC	number of components in the mixture
NG	number of groups
NGA	number of associating groups
n	number of samples analyzed
n_i	number of moles of component i or moles of associating group
n_m	total number of moles of molecules m
P	pressure (MPa)
q	surface-area segments per mole
q_j	number of surface segments assigned to group j
$\tilde{q}$	total number of surface segments
R	universal gas constant (8.314 (J K^{-1} mol^{-1}))
RD%	relative deviation $(100\sqrt{((x_{calc}-x_{\text{exp}})/x_{\text{exp}})^2})$
T	temperature (K)
T_{ci}	critical temperature of component i (K)
T^*_i	reference temperature
V	molar volume (cm^3 mol^{-1})
x	hydrocarbon mole fraction in aqueous phase
$X^{k,i}$	mole fraction of group i not bonded at site k
Y	parameter of equation (A.3)
z	number of nearest neighbors to any segment

Greek letters

α_{ij}, α_{ji}	non-randomness parameters
λ	parameter of equation (A.4)
$\Delta^{(k,I,l,j)}$	association strength between site k of group i and site l of group j (cm^3 mol^{-1})
$\varepsilon^{(k,I,l,j)}$	association energy (J)
$\kappa^{(k,I,l,j)}$	associating volume (cm^3 mol^{-1})
ν^i_j	number of type j groups in molecule i
$\nu^{(i,m)}_{assoc}$	number of associating group i in molecule m
ρ	molar density (mol cm^{-3})
ρ_j	molar density of the associating group j (mol cm^{-3})
σ_x	mean standard deviation $\sqrt{n\sum x^2-(\sum x)^2/n(n-1)}$
τ_{ij}	parameter of equation (A.9)
θ_j	surface fraction of group j

Acknowledgments

The financial support by the ECOS-SUD program and the Gas Processors Association (GPA) that provided the opportunity for this joint work is gratefully acknowledged. The authors also acknowledge the support of CONICET, Universidad Nacional del Sur and SeCyT. Javeed A. Awan wishes to thank the Higher Education Commission of Pakistan for financial support.

Appendix A

The GCA-EoS model [12–14] is based on the group contribution expression for the configurational Helmholtz function, A^c. All thermodynamic phase equilibrium properties may be derived from A^c by differentiation with respect to composition or volume.

The Helmholtz energy, A, is considered as composed of two parts, the first describes the ideal gas behavior, A^{ideal}, and the second part takes into account the intermolecular forces, that can be evaluated by a repulsive or free volume term, A^{fv}, a contribution from attractive intermolecular forces, A^{att}, and an associative term, A^{assoc}:

$$A = A^{ideal} + (A^{fv} + A^{att} + A^{assoc}) \tag{A.1}$$

The free volume contribution is modeled by assuming a hard sphere behavior for the molecules, characterizing each substance i by a hard sphere diameter d_i. A Carnahan–Starling [39] type of hard sphere expression for mixtures is adopted:

$$\left(\frac{A}{RT}\right)^{fv} = 3\left(\frac{\lambda_1\lambda_2}{\lambda_3}\right)(Y-1) + \left(\frac{\lambda_2^3}{\lambda_3^2}\right)(-Y+Y^2-\ln Y) + n\ln Y \tag{A.2}$$

with

$$Y = \left(1 - \frac{\pi\lambda_3}{6V}\right)^{-1} \tag{A.3}$$

$$\lambda_k = \sum_j^{NC} n_j d_j^k \tag{A.4}$$

where n_i is the number of moles of component i, NC stands for the number of components, V represents the total volume, R stands for universal gas constant and T is temperature.

The following, d_i, generalized expression is assumed for the hard sphere diameter temperature dependence:

$$d_i = 1.065655\, d_{ci}\left\{1 - 0.12\exp\left[-\frac{2T_{ci}}{3T}\right]\right\} \tag{A.5}$$

where d_c is the value of the hard sphere diameter at the critical temperature, T_c, for the pure component.

For the evaluation of the attractive contribution to the Helmholtz energy, a group contribution version of a density-dependent NRTL [40]-type expression is derived:

$$\left(\frac{A}{RT}\right)^{att} = -\frac{z}{2}\sum_i^{NC} n_i \sum_j^{NG} \nu_j^i q_j \sum_k^{NG} (\theta_k g_{kj}\tilde{q}\rho) / \sum_i^{NC} \theta_l \tau_{ij} \tag{A.6}$$

where

$$\theta_j = \left(\frac{q_j}{q}\right)\sum_i^{NC} n_i \nu_j^i \tag{A.7}$$

$$q = \sum_i^{NC} n_i \sum_j^{NG} \nu_j^i q_j \tag{A.8}$$

$$\tau_{ij} = \exp\left[\frac{\alpha_{ij}\Delta g_{ij}\tilde{q}}{RTV}\right] \tag{A.9}$$

$$\Delta g_{ij} = g_{ij} - g_{jj} \tag{A.10}$$

where z is the number of nearest neighbors to any segment (set to 10), NG represents number of groups, $\nu_j{}^i$ is the number of groups type j in molecule i, q_j stands for the number of surface segments assigned to group j, θ_k represents the surface fraction of group k, $\tilde{q}$ is the total number of surface segments, ρ is the molar density, g_{ij} stands for the attraction energy parameter for interactions between groups i and j, and α_{ij} is the NRTL [40] non-randomness parameter.

The interactions between unlike groups are calculated from:

$$g_{ij} = k_{ij}(g_{ii}g_{jj})^{1/2} \quad (k_{ij} = k_{ji}) \tag{A.11}$$

with the following temperature dependences for the interaction parameters:

$$g_{jj} = g_{jj}^*\left(1 + g'_{jj}\frac{T}{T_j^* - 1} + g''_{jj}\ln\frac{T}{T_j^*}\right) \tag{A.12}$$

and

$$k_{ij} = k_{ij}^*\left\{1 + k'_{ij}\ln\left[\frac{2T}{T_i^* + T_j^*}\right]\right\} \tag{A.13}$$

where g_{ij}^* and k_{ij}^* are the interaction parameters for reference temperature T_i^*, g'_{jj} and g''_{jj} represents the GCA-EoS pure-group parameters, k_{ij} and k'_{ij} stand for the GCA-EoS binary interaction parameters.

The Helmholtz function due to association is calculated with a modified form of the expression used in the SAFT equation [7,8], and is formulated in terms of associating groups:

$$\frac{A^{assoc}}{RT} = \sum_{i=1}^{NGA} n_i\left[\sum_{k=1}^{M_i}\left(\ln X^{(k,i)} - \frac{X^{(k,i)}}{2}\right) + \frac{1}{2}M_i\right] \tag{A.14}$$

where NGA represents the number of associating groups, n_i is the total number of moles of associating group i, $X^{(k,i)}$ stands for the mole fraction of group i not bonded at site k and M_i is the number of associating sites assigned to group i. The number of moles of the associating group is:

$$n_i = \sum_{m=1}^{NC} \nu_{assoc}^{(i,m)} n_m \tag{A.15}$$

where $\nu_{assoc}^{(i,m)}$ represents the number of associating group i in molecule m and n_m is the total number of moles of molecules m; the summation includes all the NC components in the mixture.

The mole fraction of group i not bonded at site k is determined by:

$$X^{(k,i)} = \left[1 + \sum_{j=1}^{NGA}\sum_{l=1}^{M_j}\rho_j X^{(i,j)}\Delta^{(k,i,l,j)}\right]^{-1} \tag{A.16}$$

$X^{(k,i)}$ depends on the molar density of the associating group j, $\rho_j = n_j/V$ and on the association strength between site k of group i and site l of group j:

$$\Delta^{(k,i,l,j)} = \frac{n_j}{V}\kappa^{(k,i,l,j)}\left[\exp\left(\frac{\varepsilon^{(k,i,l,j)}}{kT}\right) - 1\right] \tag{A.17}$$

The associating strength is function of the temperature and characteristic association parameters ε (association energy) and κ (associating volume, $cm^3\ mol^{-1}$).

References

[1] A.H. Mohammadi, D. Richon, Ind. Eng. Chem. Res. 47 (1) (2008) 7–15.
[2] A. Chapoy, A.H. Mohammadi, D. Richon, B. Tohidi, Fluid Phase Equilibr. 220 (2004) 113–121.
[3] R.A. Heidemann, J.M. Prausnitz, Proc. Natl. Acad. Sci. 73 (1976) 1773.
[4] J.R. Elliott, S.J. Suresh, M.D. Donohue, Ind. Eng. Chem. Res. 29 (7) (1990) 1476–1485.
[5] M. Wertheim, J. Stat. Phys. 42 (1986) 459–492.
[6] M. Wertheim, J. Stat. Phys. 35 (1984) 19–47.
[7] W.G. Chapman, K.E. Gubbins, G. Jackson, M. Radosz, Ind. Eng. Chem. Res. 29 (8) (1990) 1709.
[8] W.G. Chapman, K.E. Gubbins, G. Jackson, M. Radosz, Fluid Phase Equilibr. 52 (1989) 31.
[9] G.M. Kontogeorgis, M.L. Michelsen, G.K. Folas, S. Derawi, N. von Solms, E.H. Stenby, Ind. Eng. Chem. Res. 45 (14) (2006) 4855–4868.
[10] G.M. Kontogeorgis, M.L. Michelsen, G.K. Folas, S. Derawi, N. von Solms, E.H. Stenby, Ind. Eng. Chem. Res. 45 (14) (2006) 4869–4878.
[11] G.M. Kontogeorgis, E. Voutsas, I. Yakoumis, D.P. Tassios, Ind. Eng. Chem. Res. 35 (1996) 4310–4318.
[12] M.S. Zabaloy, G.D.B. Mabe, S.B. Bottini, E.A. Brignole, Fluid Phase Equilibr. 83 (1993) 159–166.
[13] H.P. Gros, S.B. Bottini, E.A. Brignole, Fluid Phase Equilibr. 116 (1996) 535–544.
[14] O. Ferreira, E.A. Brignole, E.A. Macedo, J. Chem. Thermodyn. 36 (2004) 1105–1117.
[15] I.G. Economou, C. Tsonopoulos, Chem. Eng. Sci. 52 (1997) 511–525.
[16] E.C. Voutsas, G.C. Boulougouris, I.G. Economou, D.P. Tassios, Ind. Eng. Chem. Res. 39 (3) (2000) 797–804.
[17] I.V. Yakoumis, G.M. Kontogeorgis, E.C. Voutsas, E.M. Hendriks, D.P. Tassios, Ind. Eng. Chem. Res. 37 (10) (1998) 4175–4182.
[18] M.B. Oliveira, J.A.P. Coutinho, A.J. Queimada, Fluid Phase Equilibr. 258 (2007) 58–66.
[19] A. Valtz, P. Guilbot, D. Richon, Amine BTEX Solubility, GPA Research Report 180, June 2003.
[20] S. Skjøld-Jorgensen, Ind. Eng. Chem. Res. 27 (1) (1988) 110–118.
[21] S. Skjøld-Jorgensen, Fluid Phase Equilibr. 16 (1984) 317–353.
[22] H.P. Gros, S.B. Bottini, E.A. Brignole, Fluid Phase Equilibr. 139 (1997) 75–87.

[23] S. Espinosa, G.M. Foco, A. Bermúdez, T. Fornari, Fluid Phase Equilibr. 172 (2000) 129–143.
[24] S.B. Bottini, T. Fornari, E.A. Brignole, Fluid Phase Equilibr. 158–160 (1999) 211–218.
[25] C. Tsonopoulos, Fluid Phase Equilibr. 156 (1999) 21–33.
[26] C.J. Mc Auliffe, J. Phys. Chem. 70 (4) (1966) 1267–1275.
[27] C.J. Mc Auliffe, Nature (London) 200 (1963) 1092–1093.
[28] P.J. Leinonen, D. Mackay, Can. J. Chem. Eng. 51 (1973) 230–233.
[29] I. Sanemasa, Y. Miyazaki, S. Arakawa, M. Kumamaru, T. Deguchi, Bull. Chem. Soc. Jpn. 60 (1987) 517–523.
[30] J.C. de Hemptinne, H. Delepine, C. Jose, J. Jose, Rev. Inst. Fr. Pet. 53 (4) (1998) 409–419.
[31] S. Mokraoui, C. Coquelet, A. Valtz, P.E. Hegel, D. Richon, Ind. Eng. Chem. Res. 46 (26) (2007) 9257–9262.
[32] H.D. Nelson, C.L. de Ligny, Recl. Trav. Chim. 87 (1968) 528–544.
[33] J. Polak, B.C.-Y. Lu, Can. J. Chem. 51 (230) (1973) 4018–4023.
[34] P.Y. Krasnoshchekova, M.Y. Gubergrits, Neftekhimya 13 (6) (1973) 885–888.
[35] A.N. Guseva, E.I. Parnov, Russ. J. Phys. Chem. 37 (12) (1963) 1494–11494.
[36] A.N. Guseva, E.I. Parnov, Vestn. Mosk. Univ. Khim. 19 (1) (1964) 77–78.
[37] L.A.J. Verhoeye, J. Chem. Eng. Data 13 (4) (1968) 462–467.
[38] R.A. Pierotti, A.A. Liabastre, Rep. No. ERC-0572 (1972) 1–102.
[39] N.F. Carnahan, K.E. Starling, J. Chem. Phys. 51 (1969) 635–636.
[40] H. Renon, J.M. Prausnitz, AIChE J. 14 (1968) 135–144.